

## Measurement of the Longitudinal, Transverse, and Longitudinal-Transverse Structure Functions in the ${}^2\text{H}(e, e'p)n$ Reaction

D. Jordan,<sup>1,\*</sup> T. McIlvain,<sup>1,†</sup> R. Alarcon,<sup>2</sup> R. Beck,<sup>3,‡</sup> W. Bertozzi,<sup>1</sup> V. Bhushan,<sup>1</sup> W. Boeglin,<sup>1,‡</sup> J. P. Chen,<sup>1,§</sup> D. Dale,<sup>1,||</sup> G. Dodson,<sup>1</sup> S. Dolfini,<sup>3,¶</sup> K. Dow,<sup>1</sup> J. Dzengeleski,<sup>1</sup> M. B. Epstein,<sup>4</sup> M. Farkhondeh,<sup>1</sup> S. Gilad,<sup>1</sup> J. Görgen,<sup>2</sup> M. Holtrop,<sup>1</sup> K. Joo,<sup>1</sup> J. Kelsey,<sup>1</sup> W. Kim,<sup>3</sup> R. Laszewski,<sup>3</sup> R. Lourie,<sup>5</sup> J. Mandeville,<sup>3,\*\*</sup> D. Margaziotis,<sup>4</sup> D. Martinez,<sup>2</sup> R. Miskimen,<sup>6</sup> C. N. Papanicolas,<sup>3,††</sup> S. Penn,<sup>1,‡‡</sup> W. Sapp,<sup>1</sup> A. J. Sarty,<sup>1</sup> D. Tieger,<sup>1</sup> C. Tschalaer,<sup>1</sup> W. Turchinets,<sup>1</sup> G. Warren,<sup>1</sup> L. Weinstein,<sup>1,§§</sup> and S. Williamson<sup>3</sup>

<sup>1</sup>Massachusetts Institute of Technology, Cambridge, Massachusetts 02139

<sup>2</sup>Arizona State University, Tempe, Arizona 85287

<sup>3</sup>Nuclear Physics Laboratory, University of Illinois at Urbana-Champaign, Champaign, Illinois 61820

<sup>4</sup>California State University at Los Angeles, Los Angeles, California 90032

<sup>5</sup>University of Virginia, Charlottesville, Virginia 22901

<sup>6</sup>University of Massachusetts at Amherst, Amherst, Massachusetts 01003

(Received 24 July 1995)

We have separated the longitudinal ( $f_{00}$ ), transverse ( $f_{11}$ ), and longitudinal-transverse interference ( $f_{01}$ ) structure functions in the  ${}^2\text{H}(e, e'p)n$  reaction at  $|\vec{q}| \approx 400$  MeV/c and  $\omega \approx 110$  MeV. A nonrelativistic calculation which includes effects due to final state interactions, meson exchange currents, and isobar configurations agrees with the measured  $f_{11}$  and  $f_{01}$  but overpredicts  $f_{00}$  by 25% ( $2\sigma$ ). The data are also compared to the results of previous structure function measurements.

PACS numbers: 25.30.Fj, 25.10.+s, 27.10.+h

A thorough investigation of the deuteron is of fundamental importance to nuclear physics. Many-body effects are absent in the two-nucleon system, so that the deuteron wave function can be obtained exactly given a model of the nucleon-nucleon ( $NN$ ) potential. The absence of many-body complications also permits exploration of electromagnetic currents in the deuteron via reactions involving both real and virtual photon probes. Theoretical predictions of observable effects in deuteron photodisintegration and electrodisintegration arising from meson exchange currents (MEC) and isobar configurations (IC) have been available since the latter half of the 1970s [1–3]. In addition, the effects of final state interactions (FSI) on the reaction mechanism can be calculated explicitly for deuteron electrodisintegration.

Exclusive measurements of deuteron electrodisintegration, in which an ejected particle is detected in coincidence with the scattered electron, can provide detailed information about the responses of various components of the nuclear electromagnetic current. In the first Born approximation, the electromagnetic interaction of an electron with the target nucleus is described by the exchange of a single virtual photon of four-momentum  $q_\mu = (\omega, \vec{q})$ . In this approximation, the  $(e, e'p)$  cross section can be decomposed into responses of the nuclear electromagnetic current to longitudinal and transverse polarization states of the virtual photon probe [1],

$$\frac{d^5\sigma}{d\omega^{\text{lab}} d\Omega_e^{\text{lab}} d\Omega_{np}^{\text{cm}}} = C[\rho_{00}f_{00} + \rho_{11}f_{11} + \rho_{01}f_{01} \cos(\phi_{np}^{\text{cm}}) + \rho_{-11}f_{-11} \cos(2\phi_{np}^{\text{cm}})], \quad (1)$$

where  $C$  is a function of the electron kinematics,

$$C = \frac{\alpha}{6\pi^2} \frac{1}{Q^4} \frac{k_f^{\text{lab}}}{k_i^{\text{lab}}}; \quad (2)$$

$k_i^{\text{lab}}$  ( $k_f^{\text{lab}}$ ) is the initial (final) laboratory energy of the electron,  $\alpha$  is the electromagnetic fine structure constant, and  $Q^2 = \vec{q}^2 - \omega^2$ .  $\phi_{np}^{\text{cm}}$  is the azimuthal angle (with respect to the  $z$  axis defined by  $\vec{q}$ ) of the relative  $np$  momentum in the final state.  $\phi_{np}^{\text{cm}} = 0$  or  $\pi$  corresponds to the ejected proton in the electron scattering plane. The  $\rho$ 's, which are functions of the electron kinematics only, are components of the virtual photon polarization density matrix; the subscripts 0,  $\pm 1$  denote the longitudinal and (two) transverse polarization states, respectively. Expressions for the  $\rho$ 's may be found in Ref. [1]. The structure functions  $f$ , which (for in-plane kinematics) depend only upon the momentum transfer  $q = |\vec{q}|$ , the energy transfer  $\omega$ , and the angle  $\theta_{pq}$  between the ejected proton and  $\vec{q}$ , contain all of the nuclear structure information.  $f_{00}$  and  $f_{11}$  are the longitudinal and transverse structure functions, respectively.  $f_{01}$  and  $f_{-11}$  are the longitudinal-transverse and transverse-transverse interference structure functions. It can be shown [4] that the two interference structure functions are proportional to  $\sin(\theta_{pq})$ , and thus vanish in parallel kinematics ( $\theta_{pq} = 0$ ).

Fabian and Arenhövel [1] have shown that the four structure functions have different sensitivities to the effects of FSI, MEC, and IC. In general, they show that  $f_{00}$  and  $f_{01}$  are sensitive to FSI, while  $f_{11}$  and  $f_{-11}$  are primarily sensitive to MEC and IC.

Two separations of  $f_{00}$  and  $f_{11}$  have been reported to date [5,6]. Longitudinal and transverse data measured at

NIKHEF [5] [ $0.05 \leq Q^2 \leq 0.27$  ( $\text{GeV}/c^2$ )] are underestimated by  $\sim 16\%$  on average by Arenhövel's nonrelativistic (NR) calculation and by a fully relativistic calculation by Hummel and Tjon [7]. In contrast, Arenhövel's model overpredicts  $f_{00}$  and  $f_{11}$  data taken at Saclay [6] [ $0.04 \leq Q^2 \leq 0.4$  ( $\text{GeV}/c^2$ )] by  $\sim 12\%$  on average. Measurements of  $f_{01}$  and the longitudinal-transverse asymmetry  $A_\phi$ , given by

$$A_\phi = (\sigma_0 - \sigma_\pi)/(\sigma_0 + \sigma_\pi), \quad (3)$$

where  $\sigma_0$  and  $\sigma_\pi$  are the cross sections measured at  $\phi_{np} = 0$  and  $\pi$ , respectively, have been performed at NIKHEF [8] [ $Q^2 = 0.21$  ( $\text{GeV}/c^2$ )], Saclay [6] [ $Q^2 = 0.15$  ( $\text{GeV}/c^2$ )], Bonn [9,10] [ $Q^2 = 0.18$  ( $\text{GeV}/c^2$ )], and SLAC [11] [ $Q^2 = 1.2$  ( $\text{GeV}/c^2$ )]. Arenhövel's NR calculation underpredicts  $|A_\phi|$  at missing momentum  $p_m > 100$  MeV/ $c$  by 25% to 60% for the three low- $Q^2$  data sets and by as much as a factor of 5 for the high- $Q^2$  data set. Calculations including relativistic effects performed by Hummel and Tjon, Mosconi and Ricci [3], and Arenhövel generally provide much better descriptions of the asymmetry data. Arenhövel's NR calculation similarly underpredicts the NIKHEF  $f_{01}$  data by 60% to 100% on average, while the relativistic calculation of Hummel and Tjon is once again closer to the data. In contrast, the Saclay  $f_{01}$  data are adequately described by Arenhövel's NR calculation.

We report here two sets of measurements at  $q \approx 400$  MeV/ $c$  and  $\omega \approx 110$  MeV: (1) Two measurements of the  ${}^2\text{H}(e, e'p)$  cross section performed in parallel kinematics, keeping  $q$  and  $\omega$  fixed, but varying the beam energy and scattering angles. This permits a Rosenbluth separation ["L/T (longitudinal/transverse) separation"] of  $f_{00}$  and  $f_{11}$ . (2) Two measurements of the  ${}^2\text{H}(e, e'p)$  cross section in nonparallel kinematics at  $\theta_{pq} = 11^\circ$ ,  $\phi_{np} = \pi$ , and 0. This permits extraction of  $f_{01}$ . These were the first in a series of  ${}^2\text{H}(e, e'p)$  structure function measurements using one or more out-of-plane spectrometers (OOPS) [12–14] to detect protons. The OOPS are relatively lightweight (16 tons) spectrometers designed for convenient positioning out of the electron scattering plane. In this commissioning experiment of the prototype, the OOPS was always positioned in-plane.

The experiment was performed in the North Hall of the Bates Linear Accelerator Center. The duty factor of the electron beam was about 1%, with average currents of 3 to 4  $\mu\text{A}$ . The electron beam energies were

TABLE I. Experiment kinematics (all quantities in laboratory frame).

Measurement	$k_i$ (MeV)	$k_f$ (MeV)	$\theta_e$ (deg)	$\theta_p$ (deg)	$p_f$ (MeV/ $c$ )
L/T Sep. (1)	577.1	468.5	43.7	53.9	450
L/T Sep. (2)	292.7	184.1	113.0	25.1	450
$f_{01}$ ( $\phi_{np} = 0$ )	576.0	467.0	44.0	42.9	440
$f_{01}$ ( $\phi_{np} = \pi$ )	576.0	467.0	44.0	64.7	440

measured to 1 part in  $10^3$  by the differential recoil technique, using  ${}^{12}\text{C}$  and beryllium oxide targets. Deuterated polyethylene,  $\text{CD}_2$ , spinner targets of thicknesses 49.4 and 44.3 mg/ $\text{cm}^2$  (L/T) and 77.5 mg/ $\text{cm}^2$  ( $f_{01}$ ) were used. The scattered electron and the ejected proton were detected in coincidence. The high-resolution ( $\Delta p/p \sim 10^{-4}$ ) energy loss spectrometer system (ELSSY) [15] and the prototype OOPS ( $\Delta p/p \sim 0.5 \times 10^{-2}$ ) detected and momentum analyzed electrons and protons, respectively. Table I lists the experiment kinematics. For the L/T separation, the  ${}^2\text{H}(e, e'p)$  cross section was measured at two sets of kinematics with fixed values of energy transfer,  $\omega = 109$  MeV, and momentum transfer,  $q = 402$  MeV/ $c$ . Protons of momentum  $p_f = 450$  MeV/ $c$  were detected in parallel kinematics, and thus the missing momentum,  $p_m$ , was centered at 50 MeV/ $c$  in the direction of  $\vec{q}$ . For the  $f_{01}$  measurement, the  ${}^2\text{H}(e, e'p)$  cross section was measured in nonparallel kinematics at two proton angles,  $64.7^\circ$  ( $\theta_{pq} = 10.9^\circ$ ,  $\phi_{np} = \pi$ ) and  $42.9^\circ$  ( $\theta_{pq} = 10.9^\circ$ ,  $\phi_{np} = 0$ ), for fixed electron kinematics,  $\theta_e = 44.0^\circ$ ,  $\omega = 109$  MeV, and  $q = 404$  MeV/ $c$ . The proton spectrometer central momentum was fixed at 440 MeV/ $c$ , corresponding to  $p_m = 95$  MeV/ $c$ . Note that the electron kinematics for the L/T separation and the  $f_{01}$  measurement were very similar, while  $p_m$  for the two measurements differed slightly.

The absolute efficiency for detecting electrons was established by measuring the  ${}^1\text{H}(e, e)$  cross section and comparing it to values predicted by using form factors measured and parametrized at Mainz [16]. The efficiencies at the forward and backward electron scattering angles were  $(98.4 \pm 0.2)\%$  and  $(99.1 \pm 0.3)\%$ , respectively. The absolute efficiency of the proton spectrometer was  $(97 \pm 1)\%$  (after 4%–6% corrections for known sources of dead time in OOPS), as determined by measuring  ${}^1\text{H}(e, ep)$ . In addition, the time-dependent deuterium content of the  $\text{CD}_2$  target was monitored by periodically measuring the elastic  ${}^2\text{H}(e, e)$  cross section. A 4% to 6% depletion of the deuterium content was found in each

TABLE II. Comparison of L/T data to Arenhövel's theory,  $q = 402$  MeV/ $c$ ,  $\omega = 109$  MeV,  $p_m = 50$  MeV/ $c$ .

	$\sigma$ (nb/MeV sr $^2$ )		$f_{00}$ (fm)	$f_{11}$ (fm)
	577 MeV	292 MeV		
Data	$36.1 \pm 0.5 \pm 1.0$	$4.50 \pm 0.10 \pm 0.24$	$1.78 \pm 0.07 \pm 0.15$	$1.60 \pm 0.06 \pm 0.16$
Theory	42.2	4.89	2.24	1.63
Data/theory (%)	$85.5 \pm 1.2 \pm 2.4$	$92.0 \pm 2.0 \pm 4.9$	$79.5 \pm 3.1 \pm 6.7$	$98.2 \pm 3.7 \pm 9.8$

TABLE III. Comparison of LT interference data to Arenhövel's theory,  $q = 404$  MeV/ $c$ ,  $\omega = 109$  MeV,  $p_m = 95$  MeV/ $c$ .

	$\sigma$ (nb/MeV sr <sup>2</sup> )		$f_{01}$ (fm)	$A_\phi$ (%)
	$\phi_{np} = \pi$	$\phi_{np} = 0$		
Data	$6.27 \pm 0.19 \pm 0.37$	$4.12 \pm 0.19 \pm 0.16$	$-0.116 \pm 0.014 \pm 0.016$	$-20.7 \pm 2.7 \pm 2.2$
Theory (NR)	8.30	5.98	-0.125	-16.2
Data/theory (%)	$75.5 \pm 2.3 \pm 4.5$	$68.9 \pm 3.2 \pm 2.7$	$92.8 \pm 11.2 \pm 12.8$	$128 \pm 17 \pm 14$
Theory (R)	8.21	5.41	-0.151	-20.6
Data/theory (%)	$76.4 \pm 2.3 \pm 4.5$	$76.2 \pm 3.5 \pm 3.0$	$76.8 \pm 9.3 \pm 11.3$	$100 \pm 13 \pm 11$

of the targets. Uncertainty in the measured rate of this depletion yielded uncertainties of 1.9% and 4.8% in the 577 and 292 MeV cross sections, respectively. After corrections for these various effects, the uncertainty in the knowledge of the deuterium content of the targets still dominates the uncertainty in the cross sections.

The  ${}^2\text{H}(e, e'p)$  cross sections used for the L/T separation were measured over the same ranges of  $\omega$  (104 to 112 MeV) and  $p_m$  (30 to 70 MeV/ $c$ ) for the two sets of kinematics. For the  $f_{01}$  measurement, the  $\omega$  range was 101 to 117 MeV, and the  $p_m$  range was 81 to 106 MeV/ $c$ . Radiative corrections (16% to 21%) were applied to the L/T cross sections according to Ref. [17]. For the  $f_{01}$  data, radiative corrections in nonparallel kinematics (26% to 29%) were performed using the code SIMULATE [18]. The structure functions were extracted using the kinematics determined from the central values of the spectrometer acceptances. Thus, our results represent averages over the acceptances, which was necessary to maximize the statistical precision. Tables II and III present the results of the L/T separation and the  $f_{01}$  measurements, respectively. Uncertainties are listed in the order  $\pm(\text{statistical})\pm(\text{systematic})$ . The statistical uncertainty of the structure functions is 4% for  $f_{00}$  and  $f_{11}$ , and 12% for  $f_{01}$ . The statistical uncertainty in  $A_\phi$  is 13%. The systematic uncertainties in the structure functions and the asymmetry (8% to 10% for  $f_{00}$  and  $f_{11}$ ; 14% and 11% for  $f_{01}$  and  $A_\phi$ , respectively) reflect both the uncertainties in the cross sections and in the kinematic quantities ( $k_i$  and  $\theta_e$ ) used in the separations.

We compared the cross sections and structure functions to calculations provided by Arenhövel [19]. Table II shows the ratios of the L/T data to Arenhövel's full NR (FSI + MEC + IC) calculation with the Paris [20]  $NN$  potential. The calculations have been averaged over our experimental acceptances using a Monte Carlo technique. The calculation agrees with the transverse data but overpredicts the longitudinal data by about 25% ( $2\sigma$ ). The calculated  $f_{00}$  and  $f_{11}$  at our kinematics are relatively insensitive to MEC and IC contributions ( $\leq 2\%$ ). Hence, the precision of the data is not sufficient to distinguish contributions from these small effects. But the effects of FSI (13% for  $f_{00}$ , 7% for  $f_{11}$ ) are clearly discernible and improve the agreement with the data. The spread in the calculated  $f_{00}$  and  $f_{11}$  resulting from the use of different  $NN$  potentials (Paris, Nijmegen [21], Bonn [22], and Argonne

$V_{14}$  [23]) is only about 2% to 3% at our kinematics. Again, the precision of our data is not sufficient to permit a clear discrimination among these potentials.

In Fig. 1 we compare our L/T data to results measured at Saclay [6]. The structure functions are expressed as ratios to Arenhövel's FSI + MEC + IC calculation as a function of  $p_m$ . Our  $f_{00}$  and  $f_{11}$  data agree with the trend of the Saclay data: The calculation is in good agreement with the measured transverse response, but overpredicts the longitudinal response for the points at  $p_m$  of -20, 50, and 100 MeV/ $c$ . In Fig. 2 we compare our data to the  $q = 380$  MeV/ $c$  measurements made at NIKHEF [5]. Note that our data represent averages over the range 30 to 70 MeV/ $c$  in  $p_m$ , while the NIKHEF data have been averaged over 5 MeV/ $c$  bins. Also note that the NIKHEF

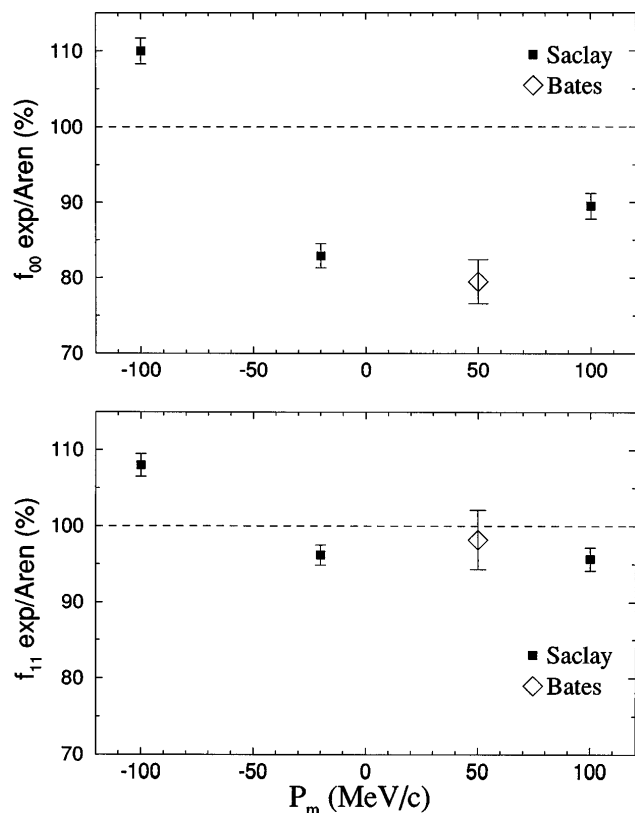


FIG. 1. Ratio of measured  $f_{00}$  and  $f_{11}$  structure functions to Arenhövel's calculation for this experiment and the Saclay experiment of Ducret *et al.* [6]. Only statistical errors are shown.

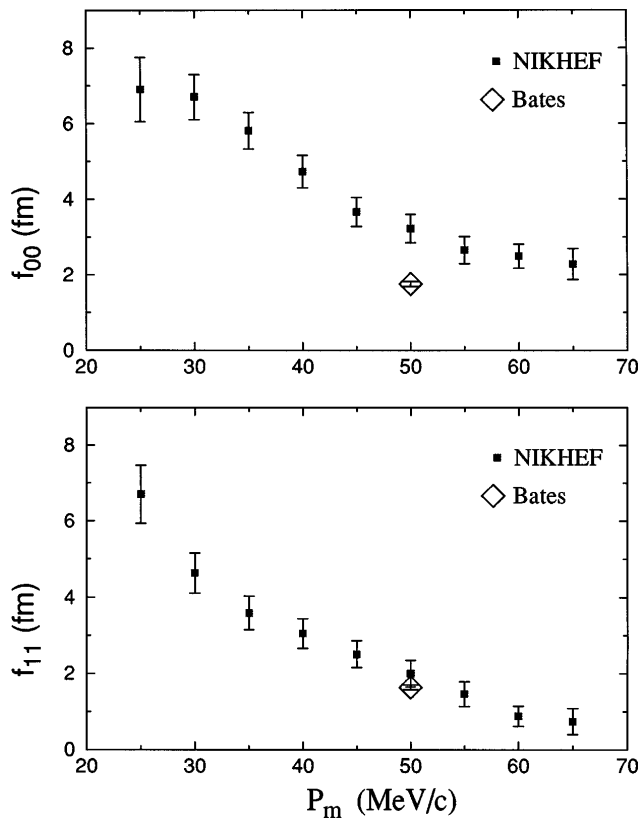


FIG. 2. Separated  $f_{00}$  and  $f_{11}$  structure functions for this experiment and the NIKHEF experiment of van der Schaar *et al.* [5]. The NIKHEF data ( $q = 380$  MeV/c) are averaged over 5 MeV/c bins in  $p_m$ . The Bates data ( $q = 400$  MeV/c) are averaged over the range of 30 to 70 MeV/c in  $p_m$ . Only statistical errors are shown.

data are at slightly different  $q$  than ours. Our transverse response agrees within statistical error with the NIKHEF measurements in the relevant  $p_m$  range. Our longitudinal response, however, lies about 40% lower than the NIKHEF data. The origin of this discrepancy is unclear.

Table III shows the ratio of the  $f_{01}$  and  $A_\phi$  data to Arenhövel's FSI + MEC + IC calculation with and without relativistic corrections. The results for  $A_\phi$  are consistent with the NIKHEF, Saclay, and Bonn results: Although the NR calculation underpredicts the absolute value of the measured  $A_\phi$ , the calculation with relativistic corrections is in good agreement with the data. For  $f_{01}$ , however, the situation is reversed: The addition of relativistic corrections worsens the agreement with the data. The NR calculation predicts the measured  $f_{01}$  within error bars, consistent with the earlier Saclay results. Thus the importance of relativistic effects in our interference data is difficult to determine unambiguously; measurements of greater statistical precision would be desirable.

We wish to acknowledge H. Arenhövel for providing us with his  ${}^2\text{H}(e, e'p)$  calculations and the technical staff of the Bates laboratory for their assistance in carrying out this work. This work was supported in part by the National Science Foundation under Grants No. NSF PHY

89-21146 and No. NSF PHY 92-00435, and the U.S. Department of Energy under Contracts No. DE-ACO2-76ERO3069 and No. DE-FG-2-88ER40415.

\*Present address: Saskatchewan Accelerator Laboratory, University of Saskatchewan, Saskatoon, Saskatchewan, Canada S7N 0W0.

†Present address: Nuclear Medicine Service, VA Medical Center, West Roxbury, MA 02132.

‡Present address: Institut für Kernphysik der Universität Mainz, W-6500 Mainz, Germany.

§Present address: Continuous Electron Beam Accelerator Facility, Newport News, VA 23606.

||Present address: University of Kentucky, Lexington, KY 40506.

¶Present address: Arizona State University, Tempe, AZ 85287.

\*\*Present address: Massachusetts General Hospital Nuclear Magnetic Resonance Center, Charlestown, MA 02129.

††Present address: National and Capodistrian University of Athens, Athens, Greece.

‡‡Present address: Nuclear Physics Laboratory, University of Washington, GL-10, Seattle, WA 98195.

§§Present address: Old Dominion University, Norfolk, VA 23529.

- [1] W. Fabian and H. Arenhövel, Nucl. Phys. **A314**, 253 (1979).
- [2] J. Laget, Phys. Lett. B **199**, 493 (1987).
- [3] B. Mosconi and P. Ricci, Nucl. Phys. **A517**, 483 (1990).
- [4] T. deForest, Ann. Phys. (N.Y.) **45**, 365 (1967).
- [5] M. van der Schaar *et al.*, Phys. Rev. Lett. **66**, 2855 (1991).
- [6] J. Ducret *et al.*, Nucl. Phys. **A553**, 697c (1993); Ph.D. thesis, Université de Paris-Sud, Orsay, France.
- [7] E. Hummel and J.A. Tjon, Phys. Rev. Lett. **63**, 1788 (1989); Phys. Rev. C **42**, 423 (1990); J. Tjon, Nucl. Phys. **A543**, 243c (1992).
- [8] M. van der Schaar *et al.*, Phys. Rev. Lett. **68**, 776 (1992).
- [9] F. Frommberger, Ph.D. thesis, Universität Bonn, Physikalisches Institut, 1993, Bonn-IR-93-63.
- [10] G. van der Steenhoven, Few Body Syst. **17**, 79 (1994).
- [11] H.J. Bulten *et al.*, Phys. Rev. Lett. **74**, 4775 (1995).
- [12] S. Dolfini *et al.*, Nucl. Instrum. Methods Phys. Res., Sect. A **344**, 571 (1994).
- [13] J. Mandeville *et al.*, Nucl. Instrum. Methods Phys. Res., Sect. A **344**, 583 (1994).
- [14] J. Mandeville *et al.*, Phys. Rev. Lett. **72**, 3325 (1994).
- [15] W. Bertozzi *et al.*, Nucl. Instrum. Methods Phys. Res. **162**, 211 (1979).
- [16] G. Simon *et al.*, Nucl. Phys. **A333**, 381 (1980).
- [17] L. Maximon, Rev. Mod. Phys. **41**, 193 (1969).
- [18] N. Makins, Ph.D. thesis, Massachusetts Institute of Technology, 1994.
- [19] H. Arenhövel (private communication).
- [20] M. Lacombe *et al.*, Phys. Rev. C **21**, 861 (1980).
- [21] M. Nagels, T. Rijken, and J. de Swart, Phys. Rev. D **17**, 768 (1978).
- [22] R. Machleidt, K. Holinde, and C. Elster, Phys. Rep. **149**, 1 (1987).
- [23] R. Wiringa, R. Smith, and T. Ainsworth, Phys. Rev. C **29**, 1207 (1984).